

On the Surprising Efficiency of Committee-based Models

Xiaofang Wang^{1,2*}
Kris M. Kitani²

Dan Kondratyuk^{1†}
Yair Movshovitz-Attias¹

Eric Christiansen¹
Elad Eban¹

¹Google Research

²Carnegie Mellon University

{xiaofan2,kkitani}@cs.cmu.edu {dankondratyuk,ericmc,yairmov,elade}@google.com

Abstract

Committee-based models, *i.e.*, model ensembles or cascades, are underexplored in recent work on developing efficient models. While committee-based models themselves are not new, there lacks a systematic understanding of their efficiency in comparison with single models. To fill this gap, we conduct a comprehensive analysis of the efficiency of committee-based models and find that committee-based models provide a complementary paradigm to achieve superior efficiency without tuning the architecture: a simple ensemble or cascade of existing networks can be considerably more efficient than state-of-the-art single models, even outperforming sophisticated neural architecture search methods. The superior efficiency of committee-based models holds true for several tasks, including image classification, video classification, and semantic segmentation, and various architecture families, such as EfficientNet, ResNet, MobileNetV2, and X3D.

1. Introduction

Optimizing the efficiency of neural networks is important for real-world applications that can only use limited computational resources or have strict requirements on response time. Recent work in this direction [43, 17, 26, 16, 33, 6] mostly focuses on designing or automatically searching for novel network architectures such that a *single* network can achieve a favorable speed-accuracy tradeoff.

On the other hand, committee-based models, *i.e.*, model ensembles or cascades, which are well-known ML techniques [2, 27, 11, 36] and are built using *multiple* models, seem to be much less used in practice. When comparing the efficiency of different methods, committee-based models are rarely considered in recent work [43, 17, 26, 16, 33, 6].

While committee-based models themselves are not new, there lacks a systematic understanding of their efficiency in

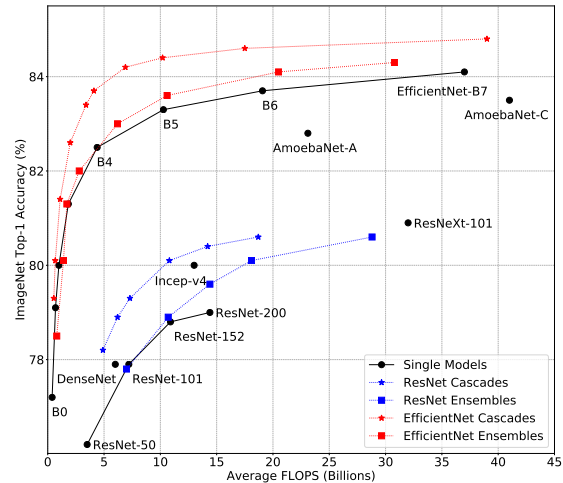


Figure 1: Committee-based models achieve a higher accuracy than single models on ImageNet while using fewer FLOPs. For example, although Inception-v4 [30] (‘Incep-v4’) outperforms all single ResNet [15] models, a ResNet cascade can still outperform Incep-v4 with fewer FLOPs.

comparison with single models that only use one network. Our work fills this gap by providing a comprehensive analysis of the efficiency of committee-based models.

Our analysis addresses the common misconceptions that ensembles or cascades: (1) are less efficient than a similarly accurate single model, or (2) require specialized techniques to achieve superior efficiency. To highlight the practical benefit of committee-based models, we intentionally choose the simplest possible method, which directly uses off-the-shelf pre-trained models to build ensembles or cascades. We ensemble multiple pre-trained models via a simple average over their predictions (Sec. 3). For model cascades, we sequentially apply each model and use a simple heuristic (*e.g.*, maximum probability in the prediction) to determine when to exit from the cascade (Sec. 4).

We find that even this method already outperforms state-of-the-art architectures found by costly neural architecture

*Work done during an internship at Google.

†Work done as part of the Google AI Residency Program.

search (NAS) methods. Note that this method works with off-the-shelf models and does not use specialized techniques for ensembles or cascades. For example, it does not require the weight generation mechanism in previous efficient ensemble methods [39], or the training of an early exit policy [1, 12] and the specially designed multi-scale architecture [18] in previous work on building cascades.

Our analysis discovers that committee-based models provide a simple complementary paradigm to achieve superior efficiency without tuning the architecture. By building ensembles or cascades of existing networks, one can obtain committee-based models that are considerably more efficient than state-of-the-art single models. We show that our findings generalize to a wide variety of tasks, including image classification, video classification, and semantic segmentation. The findings also hold true for various architecture families, *e.g.*, EfficientNet [33], ResNet [15], MobileNetV2 [26], and X3D [9].

The simplicity and superior efficiency of committee-based models make it a formidable baseline which we believe should be included in future research on designing efficient models. We emphasize that the contribution of our work is not a new method or technique but rather the comprehensive analysis and findings about the efficiency of committee-based models. These findings are informative for evaluating and advancing the research on developing efficient models. We summarize our findings as follows:

- We find that in the large computation regime, ensembles are a more cost-effective way to improve accuracy than using a single large model (Sec. 3). For example, an ensemble of two separately trained EfficientNet-B5 models matches B7 accuracy, a state-of-the-art ImageNet model, while having almost 50% less FLOPS (20.5B vs. 37B).
- We show that one can considerably speed up ensembles by converting them to cascades such that they can achieve full ensemble accuracy with a much smaller cost. Cascades outperform single models in *all* computation regimes (Sec. 4). A cascade of the two B5 models above achieves a 2.8x speedup in average FLOPS compared to B7 while retaining its accuracy (13.1B vs. 37B).
- For best performance, we show that one can design cascades to match a specific target FLOPS or accuracy by selecting models to be used in the cascade (Sec. 5.1). This yields an even higher speedup. By select existing networks from EfficientNet family, our cascade matches B7 accuracy while using on average 5.4x fewer FLOPS.
- We show that (1) the efficiency of cascades is evident in both FLOPs and in on-device throughput (Sec. 5.1); (2) cascades can provide a guarantee on worst-case FLOPS (Sec. 5.2); (3) cascades can be scaled up easily to respect different FLOPS constraints (Sec. 5.3); (4) one can build self-cascades using a single model with multiple inference resolutions to achieve a significant speedup (Sec. 6).

- We show that committee-based models are applicable beyond image classification (Sec. 7) and outperform single models on the task of video classification and semantic segmentation. Our cascade achieves a new state-of-the-art 83.1% accuracy on Kinetics-600 [5], which is 1.2% higher than X3D-XL while using fewer FLOPS.

2. Related Work

Efficient Neural Networks. There has been significant progress in designing efficient neural networks. In early work, most efficient networks, such as MobileNet [17, 26] and ShuffleNet [16], are manually designed by human experts. Recent work uses neural architectures search (NAS) to automatically learn efficient network designs [45, 4, 32, 33, 6]. They mostly improve the efficiency of single models by designing better architectures, while we explore committee-based models without tuning the architecture.

Ensembles. Ensemble learning has been well studied in machine learning and there have been many seminal works, such as Bagging [2], Boosting [27], and Adaboost [11]. Ensembles of neural networks have been used to boost the performance on many tasks, such as image classification [31, 19], machine translation [39], and out-of-distribution robustness [22, 10, 40]. But the efficiency of model ensembles has rarely been systematically investigated. Recent work indicates that model ensembles can be more efficient than single models for image classification [21, 23]. Our work further substantiates this claim through an extensive analysis of modern architectures on large-scale benchmarks.

Cascades. A large family of works have explored using cascades to speed up certain tasks. For example, the seminal work from Viola and Jones [36] builds a cascade of increasingly complex classifiers to speed up face detection. Cascades have also been explored in the context of deep neural networks. Bolukbasi et al. [1] reduces the average test-time cost by learning a policy to allow easy examples to early exit from a network. A similar idea is also explored by Guan et al. [12]. Huang et al. [18] proposes a specially designed architecture Multi-Scale DenseNet to better incorporate early exits into neural networks. Given a pool of models, Streeter [29] presents an approximation algorithm to produce a cascade such that the cascade uses minimal average inference cost to obtain a certain accuracy. Different from previous work that primarily focuses on developing new methods to build cascades, we discover that the simplest method can already provide a significant speedup, which does not require training an early exit policy [1, 12] or designing a specialized multi-scale architecture [18].

Dynamic Neural Networks. Dynamic neural networks allocate computational resources based on the input example, *i.e.*, spending more computation on hard examples and less on easy ones [14]. For example, Shazeer et al. [28]

trains a gating network to determine what parts in a high-capacity model should be used for each example. Recent work [41, 35, 38] proposes to learn a policy to dynamically select layers or blocks to execute in ResNet based on the input image. Cascades can also be viewed as dynamic neural networks and our analysis indicates that they can actually be a strong baseline for dynamic neural networks.

3. Efficiency of Ensembles

Model ensembles are useful for improving accuracy, but the usage of multiple models in an ensemble also introduces extra computational cost. When the total computation is fixed, which one will give a higher accuracy: single models or ensembles? The answer is important for real-world applications but this question has rarely been systematically studied on modern architectures and large-scale benchmarks.

To answer the question, we investigate the efficiency of ensembles on ImageNet [25] with three architecture families: EfficientNet [33], ResNet [15], and MobileNetV2 [26]. Each architecture family contains a series of networks with different levels of accuracy and computational cost. Within each family, we train a pool of models, compute the ensemble of different combinations of models, and compare these ensembles with the single models in the family.

We denote an ensemble of n image classification models by $\{M_1, \dots, M_n\}$, where M_i is the i^{th} model. Given an image x , $\alpha_i = M_i(x)$ is a vector representing the logits for each class. To ensemble the n models, we compute the mean of logits¹ $\alpha^{ens} = \frac{1}{n} \sum_i \alpha_i$ and predicts the class for image x by applying argmax to α^{ens} . The total computation of the ensemble is $\text{FLOPS}^{ens} = \sum_i \text{FLOPS}(M_i)$, where $\text{FLOPS}(\cdot)$ gives the FLOPS of a model.

We show the top-1 accuracy on ImageNet and FLOPS of single models and ensembles in Figure 2. Since there are many possible combinations of models to ensemble, we only show those Pareto optimal ensembles in the figure. We see that ensembles are more cost-effective than large single models, *e.g.*, EfficientNet-B5/B6/B7 and ResNet-152/200. But in the small computation regime, single models outperform ensembles. For example, the ensemble of 2 B5 matches B7 accuracy while using about 50% less FLOPS. However, ensembles use more FLOPS than single MobileNetV2 models when they have a similar accuracy.

We provide a possible explanation of why model ensembles are efficient at large computation but not small computation from the perspective of bias-variance tradeoff. Small models usually have small variance but large bias. Ensembles reduce the variance in prediction [44], which is already

¹We note that the mean of probabilities is a more general choice since logits can be arbitrarily scaled. In our experiments, we observe that they yield similar performance with the mean of logits being marginally better. The findings in our work hold true no matter which choice is used.

low in small models. This cannot compensate the fact that the bias of small models is large. Therefore, ensembles underperform single models at small computation. For large models, the bias is small and the variance term dominates the test error. Therefore, ensembles outperform single models at large computation by reducing the variance.

Our analysis indicates that instead of using a large model, one should use an ensemble of multiple relatively smaller models, which would give similar performance but with fewer FLOPS. In practice, model ensembles can be easily parallelized (*e.g.*, using multiple accelerators), which may provide further speedup for inference. Moreover, often the total training cost of an ensemble is much lower than that of an equally accurate single model (see supplementary materials for more details).

4. From Ensembles to Cascades

In the above we have identified the scenarios where ensembles outperform or underperform single models. Specifically, ensembles are not an ideal choice when only a small amount of computation is allowed. In this section, we show that by simply converting an ensemble to a cascade, one can significantly reduce the computation without hurting the accuracy and outperform single models in all computation regimes.

Given an input example, we need to apply all the models in an ensemble. This can be wasteful for easy input examples where a subset of models are enough to classify them correctly. Unlike ensembles, we sequentially apply models in a cascade to the input example. The prediction is progressively aggregated and early exit is allowed once the prediction is determined as highly likely to be correct. The total computation can be substantially reduced if we can accurately determine when to exit from cascades. For this purpose, we need a function to measure how likely a prediction is correct. This function is termed *confidence* and we give more details in Sec. 4.1. A formal procedure of cascades is provided in Algorithm 1.

4.1. Confidence Function

One possible choice for the confidence function is to train a policy to determine whether to move forward or stop after applying a model [1, 12]. Huang et al. [20] use the maximum probability in the predicted distribution as the confidence measure. Streeter [29] shows that the gap between the largest and second largest logits or entropy of the distribution also indicates the prediction confidence. We choose maximum probability for its simplicity.

Formally, same as above, let α be a vector representing the predicted logits. We define the confidence function $g(\cdot): \mathbb{R}^N \rightarrow \mathbb{R}$ as $g(\alpha) = \max(\text{softmax}(\alpha))$. The function $g(\cdot)$ maps predicted logits α to a confidence score. The

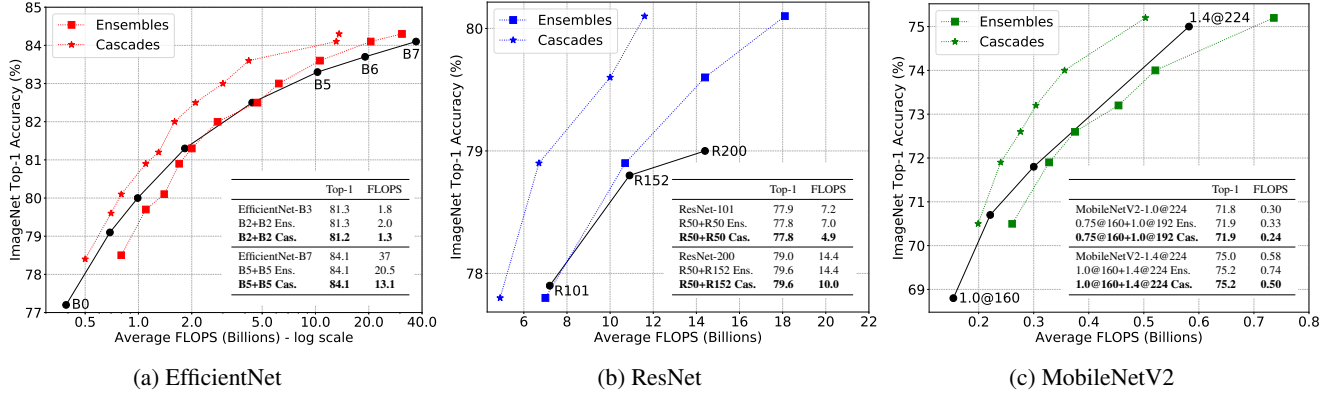


Figure 2: Ensembles outperform single models in the *large* computation regime and cascades show benefits in *all* computation regimes. Black dots represent single models in EfficientNet, ResNet or MobileNetV2. **Ensembles:** Ensembles are more cost-effective than large single models, *e.g.*, EfficientNet-B5/B6/B7 and ResNet-152/200. **Cascades:** Converting ensembles to cascades significantly reduces the FLOPS without hurting the full ensemble accuracy (each star is on the left of a square).

higher $g(\alpha)$ is, the more likely the prediction α is correct².

For a cascade of n models $\{M_i\}$, we also need $(n - 1)$ thresholds $\{t_i\}$ on the confidence score, where we use t_i to decide whether a prediction is confident enough to exit after applying model M_i (see Algorithm 1). As we define $g(\cdot)$ as the maximum probability, t_i is in $[0, 1]$. A smaller t_i indicates more images will be passed to the next model M_{i+1} . A cascade will reduce to an ensemble if all the thresholds $\{t_i\}$ are set to 1. t_n is unneeded, since the cascade will stop after applying the last model M_n , no matter how confident the prediction is.

We can flexibly control the trade-off between the computation and accuracy of a cascade through thresholds $\{t_i\}$. To understand how the thresholds influence a cascade, we visualize several 2-model cascades in Figure 3. For each cascade, we sweep t_1 from 0 and 1 and plot the results. Note that all the curves in Figure 3 have a plateau, indicating that we can significantly reduce the average FLOPS without hurting the accuracy if t_1 is properly chosen. We select the thresholds $\{t_i\}$ on held-out validation images according to the target FLOPS or validation accuracy.

4.2. Converting Ensembles to Cascades

For each ensemble in Figure 2, we convert it to a cascade that uses the same set of models. During conversion, we set the confidence thresholds such that the cascade performs similar to the ensemble while the FLOPS are minimized. By design in cascades some inputs incur more FLOPS than others. So we report the average FLOPS computed over all images in the test set.

²As a side observation, when analyzing the confidence function, we notice that models in our experiments are often slightly underconfident. This contradicts the common belief that deep neural networks tend to be overconfident [13]. Please see supplementary materials for more details.

Algorithm 1 Cascades

Input: Models $\{M_i\}$. Thresholds $\{t_i\}$. Test image x .

for $k = 1, 2, \dots, n$ **do**

$\alpha^{\text{cas}} = \frac{1}{k} \sum_{i=1}^k \alpha_i = \frac{1}{k} \sum_{i=1}^k M_i(x)$

$\text{FLOPS}^{\text{cas}} = \sum_{i=1}^k \text{FLOPS}(M_i)$

Early exit if confidence score $g(\alpha^{\text{cas}}) \geq t_k$

end for

Return α^{cas} and $\text{FLOPS}^{\text{cas}}$

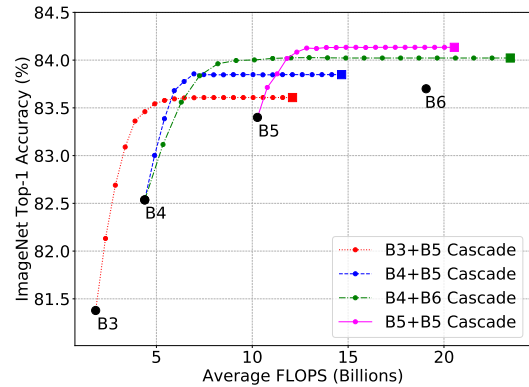


Figure 3: Cascades with different confidence thresholds. Each black dot is a single model and each square is an ensemble of models. Each colored dot represents a cascade with a specific t_1 ($0 \leq t_1 \leq 1$). As t_1 increases from 0 to 1, the cascade changes from a single model (first model in the cascade; $t_1 = 0$) to the ensemble ($t_1 = 1$). The plateau in each curve indicates that the cascade can achieve a similar accuracy to the ensemble with much less computation.

We see that cascades consistently use less computation than the original ensembles and outperform single models in all computation regimes and for all architecture families.

Taking 2 EfficientNet-B2 as an example (see Figure 2a), the ensemble initially obtains a similar accuracy to B3 but uses more FLOPS. After converting this ensemble to a cascade, we successfully reduce the average FLOPS to 1.3B (1.4x speedup over B3) and still achieve B3 accuracy. Cascades also outperform small MobileNetV2 models in Figure 2c.

5. Model Selection for Building Cascades

The cascades in Figure 2 do not optimize the choice of models and directly use the set of models in the original ensembles. For best performance, we show that one can design cascades to match a specific target FLOPS or accuracy by selecting models to be used in the cascade.

Let \mathcal{M} be the set of available models, *e.g.*, models in the EfficientNet family. Given a target FLOPS β , we select n models $M = \{M_i \in \mathcal{M}\}$ and confidence thresholds $T = \{t_i\}$ by solving the following problem:

$$\begin{aligned} \max_{\{M_i \in \mathcal{M}\}, \{t_i\}} & \text{Accuracy}(\mathcal{C}(M, T)) \\ \text{s.t.} & \text{FLOPS}(\mathcal{C}(M, T)) \leq \beta, \end{aligned} \quad (1)$$

where $\mathcal{C}(M, T)$ is the cascade of models $\{M_i\}$ with thresholds $\{t_i\}$, $\text{Accuracy}(\cdot)$ gives the validation accuracy of a cascade, and $\text{FLOPS}(\cdot)$ gives the average FLOPS. Similarly, we can also build a cascade to match a target validation accuracy γ by minimizing $\text{FLOPS}(\mathcal{C}(M, T))$ with the constraint $\text{Accuracy}(\mathcal{C}(M, T)) \geq \gamma$.

Note that this optimization is done after all models in \mathcal{M} were independently trained. The difficulty of this optimization depends on the size of \mathcal{M} and the number of models in the cascade n . The problem will be challenging if $|\mathcal{M}|$ or n is large. In our case, $|\mathcal{M}|$ and n are not prohibitive, *e.g.*, $|\mathcal{M}| = 8$ and $n \leq 4$ for EfficientNet family. We are therefore able to solve the optimization problem with exhaustive search. See supplementary materials for more details.

5.1. Targeting for a Specific FLOPS or Accuracy

For each single model, we search for a cascade to match its FLOPS (middle column in Table 1) or its accuracy (right column in Table 1). We consider all networks in the same family as the set of available models. The same model type is allowed to be used for multiple times in a cascade but they will be different models trained separately. For ImageNet experiments, the search is conducted on a small set of held-out training images and cascades are evaluated on the original validation set. We provide more experimental details in supplementary materials.

Results in Table 1 further substantiate our finding that cascades are more efficient than single models in all computation regimes. For small models, we can outperform MobileNetV2-1.0@224 by 1.4% using equivalent FLOPS. For large models, the cascade can match the accuracy of EfficientNet-B7 with only 6.9B FLOPS (a 5.4x speedup).

To better understand how a cascade works, we compute the percentage of images that exit from the cascade at each stage. The cascade above that matches B7 accuracy contains four models: [B3, B5, B5, B5]. In this cascade, 67.3% images only consume the cost of B3 and only 5.5% images use all four models. This saves a large amount of computation compared with using B7 for all the images.

Comparison with NAS. We also compare with state-of-the-art NAS methods [42, 3, 24], which can find architectures better than EfficientNet. But as shown in Table 2, a simple cascade of EfficientNet without tuning the architecture already outperforms these sophisticated NAS methods. The strong performance and simplicity of cascades should motivate future research to include them as a strong baseline when proposing novel architectures.

On-device Throughput. In the above, we use average FLOPS to measure the computational cost. We now report the throughput of cascades on TPUv3 in Table 3 to confirm that the reduction in FLOPS can translate to the real speedup on hardware. The throughput is measured as the number of images processed per second. As shown in Table 3, cascades can achieve a significant speedup over single models. Note that cascades are particularly useful for offline processing of large-scale data. For example, when processing all frames in a large video dataset, we can first apply the first model in the cascade to all frames, and then select a subset of frames based on the prediction confidence to apply following models in the cascade. In this way all the processing can be batched to fully utilize the accelerators. We provide more results in supplementary materials and show that cascades can also achieve a significant speedup for online processing.

5.2. Guarantee on Worst-case FLOPS

Up until now we have been measuring the computation of a cascade using the average FLOPS across all images. But for some images, it is possible that all the models in the cascade need to be applied. In this case, the average FLOPS cannot fully indicate the computational cost of a cascade. Therefore, we now consider worst-case FLOPS of a cascade, the sum of FLOPS of all models in the cascade.

For the three cascades in Table 1 that match the accuracy of B5, B6 or B7, we report their worst-case FLOPS in Table 4. We notice that the cascade for B7 uses fewer FLOPS than B7 in the worst-case scenario, but the cascades for B5 and B6 have higher worst-case FLOPS than the networks they compare to (see ‘w/o’ in Table 4).

We can easily find cascades with a guarantee on worst-case FLOPS by adding one more constraint on the choice of models: $\sum_i \text{FLOPS}(M_i) \leq \beta^{\text{worst}}$, where β^{worst} is the upper bound on the worst-case FLOPS of the cascade. With the new condition, we re-select models in the cascades to match of accuracy of B5 or B6. As shown in Table 4, com-

| | Single Models | | Cascades - Similar FLOPS | | | Cascades - Similar Accuracy | | |
|---------------------|---------------|-----------|--------------------------|-----------|----------------|-----------------------------|--------------|-------------|
| | Top-1 (%) | FLOPS (B) | Top-1 (%) | FLOPS (B) | Δ Top-1 | Top-1 (%) | FLOPS (B) | Speedup |
| EfficientNet | | | | | | | | |
| B1 | 79.1 | 0.69 | 80.1 | 0.67 | 1.0 | 79.3 | 0.54 | 1.3x |
| B2 | 80.0 | 1.0 | 81.2 | 1.0 | 1.2 | 80.1 | 0.67 | 1.5x |
| B3 | 81.3 | 1.8 | 82.4 | 1.8 | 1.1 | 81.4 | 1.1 | 1.7x |
| B4 | 82.5 | 4.4 | 83.7 | 4.1 | 1.2 | 82.6 | 2.0 | 2.2x |
| B5 | 83.3 | 10.3 | 84.4 | 10.2 | 1.1 | 83.4 | 3.4 | 3.0x |
| B6 | 83.7 | 19.1 | 84.6 | 17.5 | 0.9 | 83.7 | 4.1 | 4.7x |
| B7 | 84.1 | 37 | 84.8 | 39.0 | 0.7 | 84.2 | 6.9 | 5.4x |
| ResNet | | | | | | | | |
| R101 | 77.9 | 7.2 | 79.3 | 7.3 | 1.4 | 78.2 | 4.9 | 1.5x |
| R152 | 78.8 | 10.9 | 80.1 | 10.8 | 1.3 | 78.9 | 6.2 | 1.8x |
| R200 | 79.0 | 14.4 | 80.4 | 14.2 | 1.3 | 79.2 | 6.8 | 2.1x |
| MobileNetV2 | | | | | | | | |
| 1.0@160 | 68.8 | 0.154 | 69.5 | 0.153 | 0.6 | 69.1 | 0.146 | 1.1x |
| 1.0@192 | 70.7 | 0.22 | 71.8 | 0.22 | 1.1 | 70.8 | 0.18 | 1.2x |
| 1.0@224 | 71.8 | 0.30 | 73.2 | 0.30 | 1.4 | 71.8 | 0.22 | 1.4x |
| 1.4@224 | 75.0 | 0.58 | 76.1 | 0.56 | 1.1 | 75.1 | 0.43 | 1.4x |

Table 1: Cascades of EfficientNet, ResNet or MobileNetV2 models on ImageNet. The middle column shows that when using similar FLOPS, cascades can obtain a higher accuracy than single models. The right column shows that cascades can match the accuracy of single models with significantly fewer FLOPS (e.g., 5.4x fewer for B7). The benefit of cascades generalizes to all three architecture families and all computation regimes.

| | Top-1 (%) | FLOPS (B) |
|--------------------------|-------------|-----------|
| BigNASModel-L [42] | 79.5 | 0.59 |
| OFA _{Large} [3] | 80.0 | 0.60 |
| Cream-L [24] | 80.0 | 0.60 |
| Cascade* | 80.1 | 0.67 |
| BigNASModel-XL [42] | 80.9 | 1.0 |
| Cascade* | 81.2 | 1.0 |

* The cascade that matches B1 or B2 FLOPS in Table 1.

Table 2: Comparison with SOTA NAS methods. Cascades outperform single models found by costly NAS methods.

| | Top-1 (%) | Throughput (/s) | Speedup |
|----------|-----------|-----------------|-------------|
| B6 | 83.7 | 138 | |
| Cascade* | 83.7 | 415 | 3.0x |
| B7 | 84.1 | 81 | |
| Cascade* | 84.2 | 280 | 3.5x |

* The cascade that matches B6 or B7 accuracy in Table 1.

Table 3: Throughput (images processed per second) measured on TPUv3. Compared to Efficient-B6 or B7, our cascade achieves a 3.0x or 3.5x larger throughput.

pared with single models, the new cascades achieve a significant speedup in average-case FLOPS and also ensure its worst-case FLOPS are smaller. The new cascades with the guarantee on worst-case FLOPS are useful for applications with strict requirement on response time.

| | Top-1 (%) | Average-case FLOPS (B) | Worst-case FLOPS (B) | Average-case Speedup |
|-------|-----------|------------------------|----------------------|----------------------|
| B5 | 83.3 | 10.3 | 10.3 | |
| w/o* | 83.4 | 3.4 | 14.2 | 3.0x |
| with | 83.3 | 3.6 | 9.8 | 2.9x |
| B6 | 83.7 | 19.1 | 19.1 | |
| w/o* | 83.7 | 4.1 | 25.9 | 4.7x |
| with | 83.7 | 4.2 | 15.0 | 4.5x |
| B7 | 84.1 | 37 | 37 | |
| with* | 84.2 | 6.9 | 32.6 | 5.4x |

* Cascades from Table 1. The cascade for B7 was only optimized to use minimal average-case FLOPS, but it can also use fewer FLOPS than B7 in the worst-case scenario.

Table 4: Cascades can be built with a guarantee on worst-case FLOPS. We use ‘with’ or ‘w/o’ to indicate whether a cascade can provide such a guarantee or not. Cascades with such a guarantee are assured to use fewer FLOPS than single models in the worst-case scenario, and also achieve a considerable speedup in average-case FLOPS.

5.3. Cascades can be Scaled Up

One appealing property of single models is that they can be easily scaled up or down based on the available computational resources one has. We show that such property is also applicable to cascades, *i.e.*, we can scale up a base cascade to respect different FLOPS constraints. This avoids

| Model | Top-1 (%) | FLOPS (B) | Δ Top-1 | Model | Top-1 (%) | FLOPS (B) | Δ Top-1 |
|--------------------------|-------------|-------------|----------------|----------------------|-------------|-------------|----------------|
| C0 | 78.1 | 0.41 | | C3 | 82.2 | 1.8 | |
| EfficientNet-B0 [33] | 77.1 | 0.39 | 1.0 | EfficientNet-B3 [33] | 81.3 | 1.8 | 0.9 |
| C1 | 80.3 | 0.71 | | C4 | 83.7 | 4.2 | |
| EfficientNet-B1 [33] | 79.1 | 0.69 | 1.2 | EfficientNet-B4 [33] | 82.5 | 4.4 | 1.2 |
| BigNASModel-L [42] | 79.5 | 0.59 | 0.8 | C5 | 84.3 | 10.2 | |
| OFA _{Large} [3] | 80.0 | 0.60 | 0.3 | EfficientNet-B5 [33] | 83.3 | 10.3 | 1.0 |
| Cream-L [24] | 80.0 | 0.60 | 0.3 | C6 | 84.6 | 18.7 | |
| C2 | 81.2 | 1.0 | | EfficientNet-B6 [33] | 83.7 | 19.1 | 0.9 |
| EfficientNet-B2 [33] | 80.0 | 1.0 | 1.2 | C7 | 84.8 | 32.6 | |
| BigNASModel-XL [42] | 80.9 | 1.0 | 0.3 | EfficientNet-B7 [33] | 84.1 | 37 | 0.7 |

Table 5: A Family of Cascades C0 to C7. C0 to C7 significantly outperform single EfficientNet models in all computation regimes. C1 and C2 also compare favorably with state-of-the-art NAS methods [42, 3, 24]. This shows that the cascades can also be scaled up or down to respect different FLOPS constraints as single models do. This is helpful for avoiding the model selection procedure when designing cascades for different FLOPS.

| EfficientNet | Top-1 (%) | FLOPS (B) | Self-cascades | Top-1 (%) | FLOPS (B) | Speedup |
|--------------|-----------|-----------|---------------|-----------|-------------|-------------|
| B2 | 80.0 | 1.0 | B1-240-300 | 80.1 | 0.85 | 1.2x |
| B3 | 81.3 | 1.8 | B2-260-380 | 81.3 | 1.6 | 1.2x |
| B4 | 82.5 | 4.4 | B3-300-456 | 82.5 | 2.7 | 1.7x |
| B5 | 83.3 | 10.3 | B4-380-600 | 83.4 | 6.0 | 1.7x |
| B6 | 83.7 | 19.1 | B5-456-600 | 83.8 | 12.0 | 1.6x |
| B7 | 84.1 | 37 | B6-528-600 | 84.1 | 22.8 | 1.6x |

Table 6: Self-cascades. In the column of self-cascades, the two numbers represent the two resolutions r_1 and r_2 used in the cascade. Self-cascades easily outperform single models, *i.e.*, use fewer FLOPS while obtaining a similar accuracy.

the model selection procedure when designing cascades for different FLOPS, which is required for cascades in Table 1.

Specifically, we build a 3-model cascade to match the FLOPS of EfficientNet-B0. We call this cascade C0. Then, simply by scaling up the architectures in C0, we obtain a family of cascades C0 to C7 that have increasing FLOPS and accuracy. The models in C0 are from the EfficientNet family. We include more details of how we build and scale up C0 in supplementary materials. The results of C0 to C7 in Table 5 show that simply scaling up C0 gives us a family of cascades that consistently outperform single models in all computation regimes. This finding enhances the practical usefulness of cascades as one can select cascades from this family based on available resources, without worrying about what models should be used in the cascade.

6. Self-cascades

Cascades typically contain multiple models. This requires training multiple models and combining them after training. What about when only one model is available? We demonstrate that one can convert a single model into a cascade by passing the same input image at different resolutions to the model. Here, we leverage the fact that resizing an image to a higher resolution than the model is trained on often yields a higher accuracy [34] at the cost of more com-

putation. We call such cascades as “self-cascades” since these cascade only contain the model itself.

Formally, given a model M trained on the resolution r_1 , we build a 2-model cascade, where the first model is applying M to an image at resolution r_1 and the second model is applying M to the same image at resolution r_2 ($r_2 > r_1$). The idea of self-cascades generalize to three or more resolutions, but we find that two resolutions already yield satisfactory results and more resolutions yield diminishing returns.

We build self-cascades using EfficientNet models. Each EfficientNet is defined with a specific resolution (*e.g.*, 240 for B1). So, we set r_1 to its original resolution and set r_2 to a higher resolution. We set the confidence threshold such that the self-cascade matches the accuracy of a single model.

Table 6 shows that self-cascades easily outperform single models, *i.e.*, obtaining a similar accuracy with fewer FLOPS. Table 6 also suggests that if we want to obtain B7 accuracy, we can train a B6 model and then build a self-cascade, which not only uses much fewer FLOPS during inference, but also takes much shorter time to train.

Self-cascades provide a way to convert one single model to a cascade which will be more efficient than the original single model. The conversion is almost free and does not require training any additional models. They are useful when one does not have resources to train additional models or the

| | Single Models | | Cascades - Similar FLOPS | | | Cascades - Similar Accuracy | | |
|--------|---------------|-----------|--------------------------|-----------|----------------|-----------------------------|-------------|-------------|
| | Top-1 (%) | FLOPS (B) | Top-1 (%) | FLOPS (B) | Δ Top-1 | Top-1 (%) | FLOPS (B) | Speedup |
| X3D-M | 78.8 | 6.2 | 80.3 | 5.7 | 1.5 | 79.1 | 3.8 | 1.6x |
| X3D-L | 80.6 | 24.8 | 82.7 | 24.6 | 2.1 | 80.8 | 7.9 | 3.2x |
| X3D-XL | 81.9 | 48.4 | 83.1 | 38.1 | 1.2 | 81.9 | 13.0 | 3.7x |

Table 7: Cascades of X3D models on Kinetics-600. Our cascade achieves a new state-of-the-art 83.1% accuracy.

| | mIoU | FLOPS (B) | Speedup |
|---------------------|------|------------|-------------|
| ResNet-50 | 77.1 | 348 | - |
| ResNet-101 | 78.1 | 507 | - |
| Cascade - full | 78.4 | 568 | 0.9x |
| Cascade - $r = 512$ | 78.1 | 439 | 1.2x |
| Cascade - $r = 128$ | 78.2 | 398 | 1.3x |

Table 8: Cascades of DeepLabv3 models on Cityscapes.

training data is unavailable (*e.g.*, the model is downloaded).

7. Applicability beyond Image Classification

We apply cascades to tasks beyond image classification to further demonstrate its benefits. Specifically, we consider video classification on Kinetics-600 [5] and semantic segmentation on Cityscapes [8].

7.1. Video Classification

Similar to image classification, a video classification model outputs a vector of logits over possible classes. We use the same procedure as image classification to build cascades of video classification models.

We consider the X3D [9] architecture family for video classification, which is the state-of-the-art in terms of both the accuracy and efficiency. The X3D family contains a series of models of different sizes. Specifically, we build cascades of X3D models to match the FLOPS or accuracy of X3D-M, X3D-L or X3D-XL on Kinetics-600 [5].

The results are summarized in Table 7, where cascades significantly outperform the original X3D models. Our cascade outperforms X3D-XL by 1.2% while using fewer average FLOPS, and achieves 83.1% accuracy, a new state-of-the-art on Kinetics-600. Our cascade can also match the accuracy of X3D-XL with 3.7x fewer average FLOPS.

For clarity, the FLOPS in Table 7 are the inference cost for a single clip. Following Feichtenhofer [9], we sample 30 clips from each input video during inference. Please refer to supplementary materials for more experimental details.

7.2. Semantic Segmentation

In semantic segmentation, models predict a vector of logits for each pixel in the image. This differs from image

classification, where the model makes a single prediction for the entire image. We therefore revisit the confidence function definition to handle such dense prediction tasks.

Similar to before, we use the maximum probability to measure the confidence of the prediction for a single pixel p , *i.e.*, $g(\alpha_p) = \max(\text{softmax}(\alpha_p))$, where α_p is the predicted logits for pixel p . Next, we need a function $g^{\text{dense}}(\cdot)$ to rate the confidence of the dense prediction for an image, so that we can decide whether to apply the next model to this image based on this confidence score. For this purpose, we define $g^{\text{dense}}(\cdot)$ as the average confidence score of all the pixels in the image: $g^{\text{dense}}(R) = \frac{1}{|R|} \sum_{p \in R} g(\alpha_p)$, where R represents the input image.

We notice that many pixels are unlabeled in semantic segmentation datasets, *e.g.*, Cityscapes [8], and are ignored during training and evaluation. These unlabeled pixels may introduce noise when we average the confidence score of all the pixels. To filter out unlabeled pixels in the image, we only consider pixels whose confidence is higher than a preset threshold t^{unlab} . So we update the definition of $g^{\text{dense}}(\cdot)$ as follows: $g^{\text{dense}}(R) = \frac{1}{|R'|} \sum_{p \in R'} g(\alpha_p)$, where $R' = \{p \mid g(\alpha_p) > t^{\text{unlab}}, p \in R\}$.

In a cascade of segmentation models, we decide whether to pass an image R to the next model based on $g^{\text{dense}}(\cdot)$. Since the difficulty to label different parts in one image varies significantly, *e.g.*, roads are easier to segment than traffic lights, making a single decision for the entire image can be inaccurate and lead to a waste of computation. Therefore, in practice, we divide an image into grids and decide whether to pass each grid to the next model separately.

We conduct experiments on Cityscapes [8] and use mean IoU (mIoU) as the metric. We build a cascade of DeepLabv3-ResNet-50 and DeepLabv3-ResNet-101 [7] and report the results in Table 8. r is the size of the grid. The full image resolution is 1024×2048 , so $r = 512$ means each image is divided into a grid of 8 cells. We observe that if we operate on the full image level ('full'), the cascade will use more FLOPS than ResNet-101. But if operating on the grid level, the cascade can successfully reduce the computation without hurting the performance. For example, the smaller grid size (' $r = 128$ ') yields 1.3x reduction in FLOPS while matching the mIoU of ResNet-101.

8. Conclusion

We discover that committee-based models, *i.e.*, model ensembles or cascades, provide a simple complementary paradigm to obtain efficient models without tuning the architecture. Notably, model cascades achieve superior efficiency and accuracy over state-of-the-art single models on a variety of tasks. Moreover, the speedup of model cascades is evident in both FLOPS and on-device throughput. The fact that these simple committee-based models outperform sophisticated NAS methods, as well as manually designed architectures, should motivate future research to include them as strong baselines whenever presenting a new architecture. For practitioners, committee-based models outline a simple procedure to improve accuracy while maintaining efficiency that only needs off-the-shelf models.

9. Acknowledgement

The authors would like to thank Alex Alemi, Sergey Ioffe, Shankar Krishnan, Max Moroz, and Matthew Streeter for their valuable help and feedback during the development of this work. Elad and Yair would like to thank Solomonico 3rd for inspiration.

10. Contributions

Xiaofang wrote most of the code and paper, and ran all of the experiments. Elad and Yair advised on formulating the research question and plan. Dan generated the predictions of X3D on Kinetics-600. Eric conducted the experiments about the calibration of models. Kris helped in writing the paper and provided general guidance.

References

- [1] Tolga Bolukbasi, Joseph Wang, Ofer Dekel, and Venkatesh Saligrama. Adaptive neural networks for efficient inference. In *ICML*, 2017. 2, 3
- [2] Leo Breiman. Bagging predictors. *Machine learning*, 24(2):123–140, 1996. 1, 2
- [3] Han Cai, Chuang Gan, Tianzhe Wang, Zhekai Zhang, and Song Han. Once-for-all: Train one network and specialize it for efficient deployment. In *ICLR*, 2020. 5, 6, 7
- [4] Shengcao Cao, Xiaofang Wang, and Kris M. Kitani. Learnable embedding space for efficient neural architecture compression. In *ICLR*, 2019. 2
- [5] Joao Carreira, Eric Noland, Andras Banki-Horvath, Chloe Hillier, and Andrew Zisserman. A short note about kinetics-600. *arxiv:1808.01340*, 2018. 2, 8, 15
- [6] Shraman Ray Chaudhuri, Elad Eban, Hanhan Li, Max Moroz, and Yair Movshovitz-Attias. Fine-grained stochastic architecture search. *arxiv:2006.09581*, 2020. 1, 2
- [7] Liang-Chieh Chen, George Papandreou, Florian Schroff, and Hartwig Adam. Rethinking atrous convolution for semantic image segmentation. *arxiv:1706.05587*, 2017. 8, 15
- [8] Marius Cordts, Mohamed Omran, Sebastian Ramos, Timo Rehfeld, Markus Enzweiler, Rodrigo Benenson, Uwe Franke, Stefan Roth, and Bernt Schiele. The cityscapes dataset for semantic urban scene understanding. In *CVPR*, 2016. 8, 15
- [9] Christoph Feichtenhofer. X3d: Expanding architectures for efficient video recognition. In *CVPR*, 2020. 2, 8, 15
- [10] Stanislav Fort, Huiyi Hu, and Balaji Lakshminarayanan. Deep ensembles: A loss landscape perspective. *arxiv:1912.02757*, 2019. 2
- [11] Yoav Freund and Robert E Schapire. A decision-theoretic generalization of on-line learning and an application to boosting. *Journal of computer and system sciences*, 55(1):119–139, 1997. 1, 2
- [12] Jiaqi Guan, Yang Liu, Qiang Liu, and Jian Peng. Energy-efficient amortized inference with cascaded deep classifiers. In *IJCAI*, 2018. 2, 3
- [13] Chuan Guo, Geoff Pleiss, Yu Sun, and Kilian Q Weinberger. On calibration of modern neural networks. In *ICML*, 2017. 4, 12
- [14] Yizeng Han, Gao Huang, Shiji Song, Le Yang, Honghui Wang, and Yulin Wang. Dynamic neural networks: A survey. *arxiv:2102.04906*, 2021. 2
- [15] Kaiming He, Xiangyu Zhang, Shaoqing Ren, and Jian Sun. Deep residual learning for image recognition. In *CVPR*, 2016. 1, 2, 3, 11
- [16] Andrew Howard, Mark Sandler, Grace Chu, Liang-Chieh Chen, Bo Chen, Mingxing Tan, Weijun Wang, Yukun Zhu, Ruoming Pang, Vijay Vasudevan, et al. Searching for mobilenetv3. In *ICCV*, 2019. 1, 2
- [17] Andrew G Howard, Menglong Zhu, Bo Chen, Dmitry Kalenichenko, Weijun Wang, Tobias Weyand, Marco Andreetto, and Hartwig Adam. Mobilenets: Efficient convolutional neural networks for mobile vision applications. *arxiv:1704.04861*, 2017. 1, 2
- [18] Gao Huang, Danlu Chen, Tianhong Li, Felix Wu, Laurens van der Maaten, and Kilian Q Weinberger. Multi-scale dense networks for resource efficient image classification. In *ICLR*, 2018. 2
- [19] Gao Huang, Yixuan Li, Geoff Pleiss, Zhuang Liu, John E Hopcroft, and Kilian Q Weinberger. Snapshot ensembles: Train 1, get m for free. In *ICLR*, 2017. 2
- [20] Gao Huang, Zhuang Liu, Laurens Van Der Maaten, and Kilian Q Weinberger. Densely connected convolutional networks. In *CVPR*, 2017. 3
- [21] Dan Kondratyuk, Mingxing Tan, Matthew Brown, and Boqing Gong. When ensembling smaller models is more efficient than single large models. *arxiv:2005.00570*, 2020. 2
- [22] Balaji Lakshminarayanan, Alexander Pritzel, and Charles Blundell. Simple and scalable predictive uncertainty estimation using deep ensembles. In *NeurIPS*, 2017. 2
- [23] Ekaterina Lobacheva, Nadezhda Chirkova, Maxim Kodryan, and Dmitry P Vetrov. On power laws in deep ensembles. In *NeurIPS*, 2020. 2
- [24] Houwen Peng, Hao Du, Hongyuan Yu, Qi Li, Jing Liao, and Jianlong Fu. Cream of the crop: Distilling prioritized paths for one-shot neural architecture search. In *NeurIPS*, 2020. 5, 6, 7

- [25] Olga Russakovsky, Jia Deng, Hao Su, Jonathan Krause, Sanjeev Satheesh, Sean Ma, Zhiheng Huang, Andrej Karpathy, Aditya Khosla, Michael Bernstein, et al. Imagenet large scale visual recognition challenge. *IJCV*, 2015. [3](#)
- [26] Mark Sandler, Andrew Howard, Menglong Zhu, Andrey Zhmoginov, and Liang-Chieh Chen. Mobilenetv2: Inverted residuals and linear bottlenecks. In *CVPR*, 2018. [1](#), [2](#), [3](#), [11](#)
- [27] Robert E Schapire. The strength of weak learnability. *Machine learning*, 5(2):197–227, 1990. [1](#), [2](#)
- [28] Noam Shazeer, Azalia Mirhoseini, Krzysztof Maziarz, Andy Davis, Quoc Le, Geoffrey Hinton, and Jeff Dean. Outrageously large neural networks: The sparsely-gated mixture-of-experts layer. In *ICLR*, 2017. [2](#)
- [29] Matthew Streeter. Approximation algorithms for cascading prediction models. In *ICML*, 2018. [2](#), [3](#), [14](#)
- [30] Christian Szegedy, Sergey Ioffe, Vincent Vanhoucke, and Alex Alemi. Inception-v4, inception-resnet and the impact of residual connections on learning. In *AAAI*, 2017. [1](#)
- [31] Christian Szegedy, Wei Liu, Yangqing Jia, Pierre Sermanet, Scott Reed, Dragomir Anguelov, Dumitru Erhan, Vincent Vanhoucke, and Andrew Rabinovich. Going deeper with convolutions. In *CVPR*, 2015. [2](#)
- [32] Mingxing Tan, Bo Chen, Ruoming Pang, Vijay Vasudevan, Mark Sandler, Andrew Howard, and Quoc V Le. Mnasnet: Platform-aware neural architecture search for mobile. In *CVPR*, 2019. [2](#)
- [33] Mingxing Tan and Quoc Le. Efficientnet: Rethinking model scaling for convolutional neural networks. In *ICML*, 2019. [1](#), [2](#), [3](#), [7](#), [11](#), [14](#)
- [34] Hugo Touvron, Andrea Vedaldi, Matthijs Douze, and Hervé Jégou. Fixing the train-test resolution discrepancy. In *NeurIPS*, 2019. [7](#)
- [35] Andreas Veit and Serge Belongie. Convolutional networks with adaptive inference graphs. In *ECCV*, 2018. [3](#)
- [36] Paul Viola and Michael Jones. Rapid object detection using a boosted cascade of simple features. In *CVPR*, 2001. [1](#), [2](#)
- [37] Neal Wadhwa, Rahul Garg, David E Jacobs, Bryan E Feldman, Nori Kanazawa, Robert Carroll, Yair Movshovitz-Attias, Jonathan T Barron, Yael Pritch, and Marc Levoy. Synthetic depth-of-field with a single-camera mobile phone. *ACM Transactions on Graphics (TOG)*, 37(4):1–13, 2018. [11](#)
- [38] Xin Wang, Fisher Yu, Zi-Yi Dou, Trevor Darrell, and Joseph E Gonzalez. Skipnet: Learning dynamic routing in convolutional networks. In *ECCV*, 2018. [3](#)
- [39] Yeming Wen, Dustin Tran, and Jimmy Ba. Batchensemble: an alternative approach to efficient ensemble and lifelong learning. In *ICLR*, 2020. [2](#)
- [40] Florian Wenzel, Jasper Snoek, Dustin Tran, and Rodolphe Jenatton. Hyperparameter ensembles for robustness and uncertainty quantification. In *NeurIPS*, 2020. [2](#)
- [41] Zuxuan Wu, Tushar Nagarajan, Abhishek Kumar, Steven Rennie, Larry S Davis, Kristen Grauman, and Rogerio Feris. Blockdrop: Dynamic inference paths in residual networks. In *CVPR*, 2018. [3](#)
- [42] Jiahui Yu, Pengchong Jin, Hanxiao Liu, Gabriel Bender, Pieter-Jan Kindermans, Mingxing Tan, Thomas Huang, Xiaodan Song, Ruoming Pang, and Quoc Le. Bignas: Scaling up neural architecture search with big single-stage models. In *ECCV*, 2020. [5](#), [6](#), [7](#)
- [43] Xiangyu Zhang, Xinyu Zhou, Mengxiao Lin, and Jian Sun. Shufflenet: An extremely efficient convolutional neural network for mobile devices. In *CVPR*, 2018. [1](#)
- [44] Zhi-Hua Zhou. *Ensemble methods: foundations and algorithms*. CRC press, 2012. [3](#)
- [45] Barret Zoph, Vijay Vasudevan, Jonathon Shlens, and Quoc V Le. Learning transferable architectures for scalable image recognition. In *CVPR*, 2018. [2](#)

A. On-device Throughput and Latency

We report the on-device throughput and latency of cascades to confirm that the reduction in FLOPS can translate to the real speedup on hardware. The throughput or latency of a model is highly dependent on the batch size. So we consider two scenarios: (1) offline processing, where we can batch the examples, and (2) online processing, where we use a fixed batch size 1.

Offline Processing. Cascades are particularly useful for offline processing of large-scale data. For example, when processing all frames in a large video dataset, we can first apply the first model in the cascade to all frames, and then select a subset of frames based on the prediction confidence to apply following models in the cascade. In this way all the processing can be batched to fully utilize the accelerators. We report the throughput of cascades on TPUv3 in Table A, which is measured as the number of images processed per second. We use batch size 16 when running models on TPUv3 for the case of offline processing. As shown in Table A, cascades achieve a much larger throughput than single models while being equally accurate.

Online Processing. Cascades are also useful for online processing with a fixed batch size 1. Using batch size 1 is sub-optimal for the utilization of accelerators like GPU or TPU, but it still happens in some real-world applications, *e.g.*, robots processing one frame at a time or mobile phone cameras processing a single image [37]. We report the average latency of cascades on TPUv3 with batch size 1 in Table B. We see that cascades achieve a similar accuracy to single models but use a much smaller average latency to return the prediction.

B. Efficiency of Ensembles

B.1. Training Time of Ensembles

In Sec. 3, we show that ensembles match the accuracy of large single models with fewer inference FLOPS. We now show that the total training cost of an ensemble can also be lower than an equally accurate single model.

We show the training time of single EfficientNet models in Table C. We use 32 TPUv3 cores to train B0 to B5, and 128 TPUv3 cores to train B6 or B7. All the models are trained with the public official implementation of EfficientNet. We choose the ensemble that matches the accuracy of B6 or B7 and compute the total training time of the ensemble based on Table C. As shown in Table D, the ensemble of 2 B5 can match the accuracy of B7 while being faster in both training and inference.

B.2. Experimental Details

When analyzing the efficiency of ensembles, we conduct experiments on three architecture families: EfficientNet [33], ResNet [15] and MobileNetV2 [26]. The Effi-

| | Top-1 (%) | Throughput (/s) | Speedup |
|----------|-----------|-----------------|-------------|
| B1 | 79.1 | 1436 | |
| Cascade* | 79.3 | 1798 | 1.3x |
| B2 | 80.0 | 1156 | |
| Cascade* | 80.1 | 1509 | 1.3x |
| B3 | 81.3 | 767 | |
| Cascade* | 81.4 | 1111 | 1.4x |
| B4 | 82.5 | 408 | |
| Cascade* | 82.6 | 656 | 1.6x |
| B5 | 83.3 | 220 | |
| Cascade* | 83.4 | 453 | 2.1x |
| B6 | 83.7 | 138 | |
| Cascade* | 83.7 | 415 | 3.0x |
| B7 | 84.1 | 81 | |
| Cascade* | 84.2 | 280 | 3.5x |

* The cascade that matches the accuracy of EfficientNet-B1 to B7 in the right column if Table 1.

Table A: Throughput on TPUv3 for the case of offline processing. Throughput is measured as the number of images processed per second. Cascades achieve a much larger throughput than single models while being equally accurate.

| | Top-1 (%) | Latency (ms) | Speedup |
|----------|-----------|--------------|-------------|
| B1 | 79.1 | 3.7 | |
| Cascade* | 79.3 | 3.0 | 1.2x |
| B2 | 80.0 | 5.2 | |
| Cascade* | 80.1 | 3.7 | 1.4x |
| B3 | 81.3 | 9.7 | |
| Cascade* | 81.4 | 5.9 | 1.7x |
| B4 | 82.5 | 16.6 | |
| Cascade* | 82.6 | 9.6 | 1.7x |
| B5 | 83.3 | 27.2 | |
| Cascade* | 83.4 | 14.3 | 1.9x |
| B6 | 83.7 | 57.1 | |
| Cascade* | 83.7 | 15.1 | 3.8x |
| B7 | 84.1 | 126.6 | |
| Cascade* | 84.2 | 23.2 | 5.5x |

* The cascade that matches the accuracy of EfficientNet-B1 to B7 in the right column if Table 1.

Table B: Average latency on TPUv3 for the case of online processing with batch size 1. Cascades are much faster than single models in terms of the average latency while being similarly accurate.

| B0 | B1 | B2 | B3 | B4 | B5 | B6 | B7 |
|----|----|----|----|----|----|-----|-----|
| 9 | 12 | 15 | 24 | 32 | 48 | 128 | 160 |

Table C: Training time (TPUv3 days) of EfficientNet.

| | Top-1 (%) | FLOPS (B) | Training |
|----------|-----------|-----------|----------|
| B6 | 83.7 | 19.1 | 128 |
| B3+B4+B4 | 83.6 | 10.6 | 88 |
| B7 | 84.1 | 37 | 160 |
| B5+B5 | 84.1 | 20.5 | 96 |
| B5+B5+B5 | 84.3 | 30.8 | 144 |

Table D: Training time (TPU v3 days) of ensembles. We use the ‘+’ notation to indicate the models in ensembles. Ensembles are faster than single models in both training and inference while achieve a similar accuracy.

cientNet family consists of eight networks: EfficientNet-B0 to B7. We consider four networks in the ResNet family: ResNet-50/101/152/200. For MobileNetV2, we consider MobileNetV2-0.75@160, 1.0@160, 1.0@192, 1.0@224, and 1.4@224. Each MobileNetV2 network is represented in the form of $w@r$, where w is the width multiplier and r is the image resolution.

For EfficientNet, we consider ensembles of two to four models of either the same or different architectures. When the same architecture is used multiple times in an ensemble, *e.g.*, B5 and B5, they are different models trained separately from different random initializations. The FLOPS range of ResNet or MobileNetV2 models is relatively narrow compared to EfficientNet, so we only consider ensembles of two models for ResNet and MobileNetV2.

C. From Ensembles to Cascades

C.1. Confidence Function

We empirically show that the higher the confidence score $g(\alpha)$ is, the more likely the prediction given by α is correct. In Sec 4.1, we define the confidence function as the maximum probability in the predicted distribution. Other than that, the following metrics can also indicate the prediction confidence: the gap between the largest and second largest logits, the gap between the largest and second largest probabilities, and the (negative) entropy of the distribution.

Given a set of images, we select the top- $k\%$ images with highest confidence scores. Then we compute the classification accuracy within the selected images. If a higher confidence score indicates that the prediction is more likely to be correct, the accuracy should drop as k increases. For a EfficientNet-B0 model trained on ImageNet, we sweep k from 0 to 100 and compute the accuracy within the selected

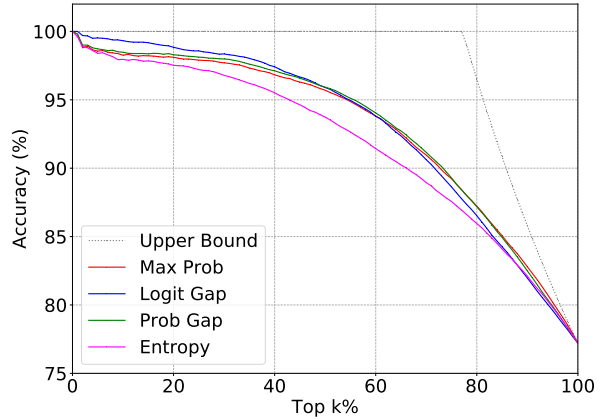


Figure A: Different metrics for the confidence function. When $k = 100$, all the images are selected so the accuracy is exactly the accuracy of EfficientNet-B0 (77.1%). The ‘Upper Bound’ curve represents the best possible performance for the metric. It has 100% accuracy when $k \leq 77.1$, *i.e.*, all the selected images are correctly classified. The accuracy starts to drop when k becomes larger, since some misclassified images are inevitably chosen.

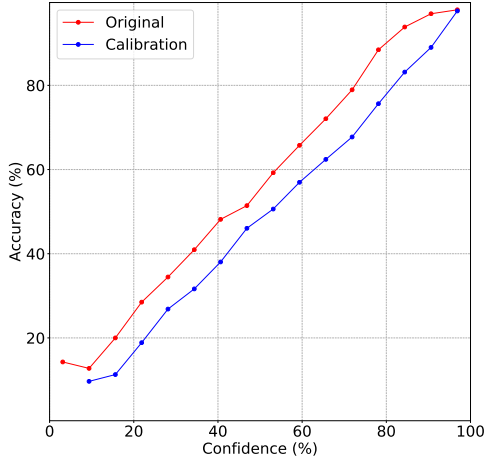
top- $k\%$ images from the ImageNet validation set.

As shown in Figure A, the accuracy drops as more images are selected. This empirically shows that predictions with a higher confidence score are more likely to be correct. All the metrics demonstrate reasonably good performance, where the entropy performs slightly worse than other metrics. The logit gap performs the best when $k < 60$. When k becomes larger, the maximum probability and probability gap performs the best.

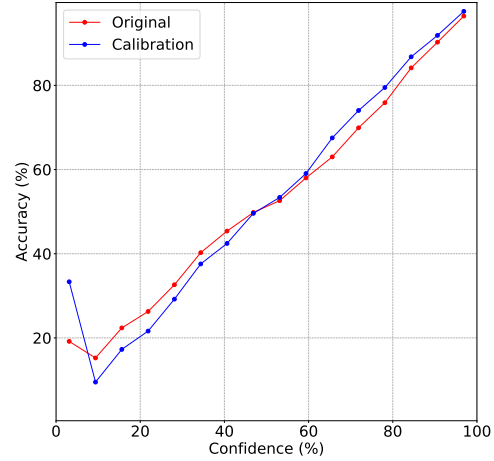
C.2. Calibration of Models

As a side observation, when analyzing the confidence function, we notice that models in our experiments are often slightly underconfident, *i.e.*, the confidence p is slightly lower than the actual accuracy of images whose prediction confidence is p (see the ‘Original’ curve in Figure B). This observation contradicts the common belief that deep neural networks tend to be overconfident [13]. Here, the confidence of a prediction is defined as the probability associated with the predicted class [13], which is equivalent to the maximum probability in the predicted distribution.

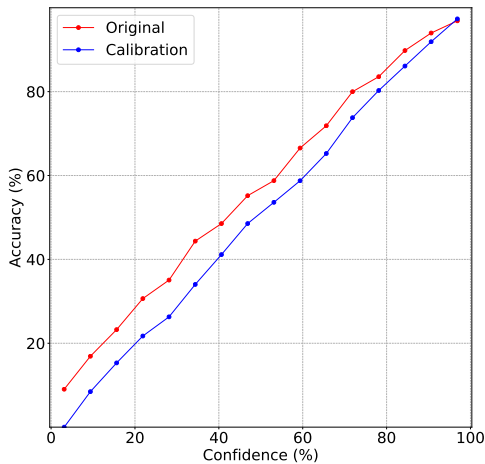
A model is considered as calibrated if the confidence of its prediction correctly estimates the true correctness likelihood (neither overconfident nor underconfident). The calibration of models can influence the ensemble performance when we ensemble models via simple averaging. If models in an ensemble are poorly calibrated, overconfident models may dominate the prediction, making those underconfident models useless in the ensemble.



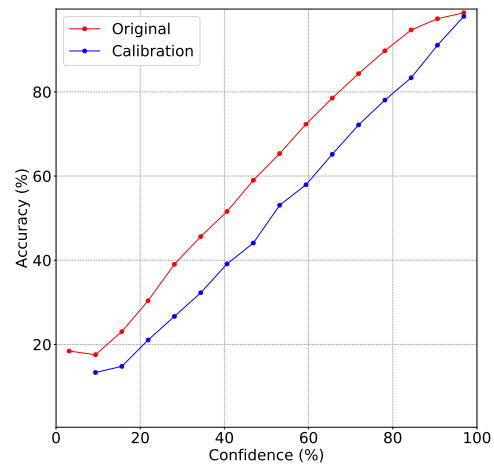
(a) EfficientNet-B3



(b) ResNet-50



(c) MobileNet-1.0@192



(d) X3D-M

Figure B: Confidence vs. accuracy for EfficientNet-B3, ResNet-50, MobileNet-1.0@192, and X3D-M on their respective dataset. ‘Original’ refers to the original prediction and ‘Calibration’ refers to the prediction after calibration. We divide the confidence into several intervals. Then for each interval, we visualize the accuracy of images whose confidence is within this interval. The original prediction is slightly underconfident, *i.e.*, the confidence p is slightly lower than the actual accuracy of images whose prediction confidence is p . After calibration, the confidence almost equals to the actual accuracy.

For models in our experiments, we also have tried calibrating them before computing the ensemble performance. To calibrate a model, we use Platt scaling via a learned monotonic calibration network. As shown in the ‘Calibration’ curve in Figure B, the calibration improves the connection between the prediction confidence and accuracy, *i.e.*, the confidence after calibration almost equals to the actual accuracy. But we also notice that calibrating models only has a small influence on the final ensemble performance in our experiments, which might be because these models are just slightly underconfident before calibration. Therefore, we do not calibrate any model when computing the ensemble in all our experiments.

C.3. Determine the Thresholds

Given the n models $\{M_i\}$ in a cascade, we also need $(n - 1)$ thresholds $\{t_i\}$ on the confidence score. We can flexibly control the trade-off between the computation and accuracy of a cascade through thresholds $\{t_i\}$.

We determine the thresholds $\{t_i\}$ based on the target FLOPS or accuracy on validation images. Note that the thresholds are determined after all models are trained. We only need the logits of validation images to determine $\{t_i\}$, so computing the cascade for a specific choice of thresholds is fast. Therefore we can select the thresholds by enumerating all possible combinations for $\{t_i\}$. As t_i is a real number, we make sure two trials of t_i are sufficiently differ-

ent by only considering the percentiles of confidence scores as possible values. When $n > 2$, there might be multiple choices of $\{t_i\}$ that can give the target FLOPS or accuracy. In that case, we choose $\{t_i\}$ that gives the higher accuracy or fewer FLOPS. Many choices for $\{t_i\}$ can be easily ruled out as the FLOPS or accuracy of a cascade changes monotonically with respect to any threshold t_i .

In practice, we often want the accuracy of a cascade to match the accuracy of a single model. To do that, we determine the thresholds such that the cascade matches the accuracy of the single model on *validation* images. Such thresholds usually enable the cascade to have a similar *test* accuracy to the single model.

For ImageNet, we randomly select $\sim 25k$ training images and exclude them from training. We use these held-out training images to determine the confidence thresholds. The final accuracy is computed on the original ImageNet validation set.

D. Model Selection for Building Cascades

D.1. Targeting for a Specific FLOPS or Accuracy

We can build cascades to match a specific FLOPS or accuracy by optimizing the choice of models and confidence thresholds, *e.g.*, solving Eq. 1 when targeting for a specific FLOPS. Note that this optimization is done after all models in M are trained. The optimization complexity is exponential in $|\mathcal{M}|$ and n , and the problem will be challenging if $|\mathcal{M}|$ and n are large. In our experiments, $|\mathcal{M}|$ and n are not prohibitive. Therefore, we solve the optimization problem with exhaustive search. One can also use more efficient procedures such as the algorithm described in [29].

Concretely, for EfficientNet, $|\mathcal{M}| = 8$ and $n \leq 4$; for ResNet, $|\mathcal{M}| = 4$ and $n = 2$; for MobileNetV2, $|\mathcal{M}| = 5$ and $n = 2$. The networks in each family are the same as listed in Sec. B.2. We do not consider cascades of more than four EfficientNet models because we observe diminishing returns as n increases. Same as ensembles in Sec B.2, we only consider cascades of two ResNet or MobileNetV2 models due to their relative narrow FLOPS range.

We allow the same network to be used by multiple times in one cascade but they will be different models trained separately. Taking EfficientNet for an example, we have in total 4672 ($= 8^4 + 8^3 + 8^2$) possible combinations of models. In practice, we first train each EfficientNet model separately for four times and pre-compute their predicted logits. Then for each possible combination of models, we load the logits of models and determine the thresholds according to the target FLOPS or accuracy. Finally, we choose the best cascade among all possible combinations. Similar as above, we choose models and thresholds on held-out training images for ImageNet experiments. No images from the ImageNet validation set are used when we select models for a cascade.

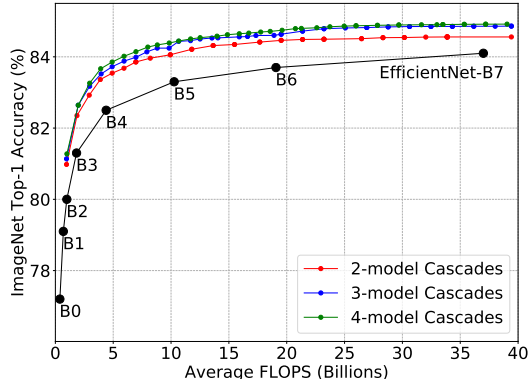


Figure C: Impact of the number of models in cascades.

D.2. Cascades can be Scaled Up

The networks in EfficientNet family are obtained by scaling up the depth, width and resolution of B0. The scaling factors for depth, width and resolution are defined as $d = \alpha^\phi$, $w = \beta^\phi$ and $r = \gamma^\phi$, respectively, where $\alpha = 1.2$, $\beta = 1.1$ and $\gamma = 1.15$, as suggested in Tan et al. [33]. One can control the network size by changing ϕ . For example, $\phi = 0$ gives B0, $\phi = 1$ gives B2, and $\phi = 7$ gives B7.

We build a 3-model cascade C0 that matches the FLOPS of EfficientNet-B0 by solving Eq. 1 on held-out training images from ImageNet. When building C0, we consider 13 networks from EfficientNet family. As we want C0 to use similar FLOPS to B0, we make sure the 13 networks include both networks smaller than B0 and networks larger than B0. Their ϕ are set to -4.0, -3.0, -2.0, -1.0, 0.0, 0.25, 0.5, 0.75, 1.0, 1.25, 1.50, 1.75, 2.0, respectively.

The ϕ of the three models in C0 are -2.0, 0.0 and 0.75. Then simply scaling up the architectures in C0, *i.e.*, increasing the ϕ of each model in C0, gives us a family of cascades C0 to C7 that have increasing FLOPS and accuracy. The thresholds in C0 to C7 are determined such that their FLOPS are similar to B0 to B7.

D.3. Exit Ratios

To better understand how a cascade works, we compute the exit ratio of the cascade, *i.e.*, the percentage of images that exit from the cascade at each stage. Specifically, we choose the cascades in Table 1&4 that match the accuracy of B1 to B7 and report their exit ratios in Table E. For all the cascades in Table E, most images only consume the cost of the first model in the cascade and only a few images have to use all the models. This shows that cascades are able to allocate fewer resources to easy images and explains the speedup of cascades over single models.

| | Top-1 (%) | FLOPS (B) | Exit Ratio (%) at Each Stage | | | |
|--------------|-----------|-----------|------------------------------|---------|---------|---------|
| | | | Model 1 | Model 2 | Model 3 | Model 4 |
| B1 | 79.1 | 0.69 | | | | |
| B0+B1 | 79.3 | 0.54 | 78.7 | 21.3 | | |
| B2 | 80.0 | 1.0 | | | | |
| B0+B1+B3 | 80.1 | 0.67 | 73.2 | 21.4 | 5.4 | |
| B3 | 81.3 | 1.8 | | | | |
| B0+B3+B3 | 81.4 | 1.1 | 68.0 | 26.4 | 5.7 | |
| B4 | 82.5 | 4.4 | | | | |
| B1+B3+B4 | 82.6 | 2.0 | 67.9 | 15.3 | 16.8 | |
| B5 | 83.3 | 10.3 | | | | |
| B2+B4+B4+B4 | 83.4 | 3.4 | 67.6 | 21.2 | 0.0 | 11.2 |
| B2+B4+B4* | 83.3 | 3.6 | 57.7 | 26.0 | 16.3 | |
| B6 | 83.7 | 19.1 | | | | |
| B2+B4+B5+B5 | 83.7 | 4.1 | 67.6 | 21.2 | 5.9 | 5.3 |
| B3+B4+B4+B4* | 83.7 | 4.2 | 67.3 | 16.2 | 10.9 | 5.6 |
| B7 | 84.1 | 37 | | | | |
| B3+B5+B5+B5* | 84.2 | 6.9 | 67.3 | 21.6 | 5.6 | 5.5 |

* Cascades from Table 4 with a guarantee on worstcase FLOPS.

Table E: Exit ratios of cascades. We use the ‘+’ notation to indicate the models in cascades.

D.4. Number of Models in Cascades

We study the influence of the number of models in cascades on the performance. Concretely, we consider the EfficientNet family and follow the same experimental setup as in Sec. D.1. We sweep the target FLOPS from 1 to 40 and find cascades of 2, 3 or 4 models. As shown in Figure C, the performance of cascades keeps improving as the number of models increases. We see a big gap between 2-model cascades and 3-model cascades, but increasing the number of models from 3 to 4 demonstrates a diminishing return.

E. Applicability beyond Image Classification

E.1. Video Classification

For video classification, we conduct experiments on Kinetics-600 [5]. Following Feichtenhofer [9], we sample 30 clips from each input video when evaluating X3D models on Kinetics-600. The 30 clips are the combination of 10 uniformly sampled temporal crops and 3 spatial crops. The final prediction is the mean of all individual predictions. The FLOPS in Table 5 are the inference cost for a single clip, so the total FLOPS for single models or cascades need to be multiplied by 30. We omit ‘ $\times 30$ ’ in Table 5 for brevity. This does not change the relative speedup of cascades over single models.

E.2. Semantic Segmentation

For semantic segmentation, we conduct experiments on the Cityscapes [8] dataset, where the full image resolution is 1024×2048 . We train DeepLabv3 [7] models on the train set of Cityscapes and report the mean IoU (mIoU) over classes on the validation set. The threshold t^{unlab} to filter out unlabeled pixels is set to 0.5. For DeepLabv3-ResNet-50 or DeepLabv3-ResNet-101, we follow the original architecture of ResNet-50 or ResNet-101, except that the first 7×7 convolution is changed to three 3×3 convolutions.